OncoTargets and Therapy

Dovepress
open access to scientific and medical research

Open Access Full Text Article

ORIGINAL RESEARCH

Sympathetic innervation contributes to perineural invasion of salivary adenoid cystic carcinoma via the β2-adrenergic receptor

This article was published in the following Dove Medical Press journal:
OncoTargets and Therapy

Chao Ma,[1,*] Tao Gao,[1,2,*] Jun Ju,[3,*] Yi Zhang,[4] Qianwei Ni,[5] Yun Li,[1] Zhenyan Zhao,[1] Juan Chai,[6] Xiangming Yang,[1] Moyi Sun[1]

[1]State Key Laboratory of Military Stomatology, National Clinical Research Center for Oral Diseases, Shaanxi Clinical Research Center for Oral Diseases, Department of Oral and Maxillofacial Surgery, School of Stomatology, The Fourth Military Medical University, Xi'an, Shaanxi, China; [2]Department of Stomatology, The First Hospital of Yu Lin, Yu Lin, Shaanxi, China; [3]Department of Otolaryngology Head and Neck Surgery, Navy General Hospital, Beijing, China; [4]Department of Geriatrics, School of Stomatology, The Fourth Military Medical University, Xi'an, Shaanxi, China; [5]Department of Oral and Maxillofacial Surgery, General Hospital of Xinjiang Military Region, Urumqi, Xin Jiang, China; [6]Department of Oral and Maxillofacial Surgery, School of Stomatology, Xi'an Medical University, Xi'an, Shaanxi, China

*These authors contributed equally to this work

Correspondence: Moyi Sun
State Key Laboratory of Military Stomatology, National Clinical Research Center for Oral Diseases, Shaanxi Clinical Research Center for Oral Diseases, Department of Oral and Maxillofacial Surgery, School of Stomatology, The Fourth Military Medical University, 145 West Changle Road, Xi'an, Shaanxi 710032, China
Tel +86 139 9117 6800
Email moyisun@163.com

Purpose: Perineural invasion (PNI) is reported to correlate with local recurrence and poor prognosis of salivary adenoid cystic carcinoma (SACC). However, the pathogenesis of PNI remains unclear. The aims of this study were to investigate the correlation between sympathetic innervation and SACC PNI and to elucidate how the sympathetic neurotransmitter norepinephrine (NE) regulates the PNI process.

Materials and methods: Sympathetic innervation and β2-adrenergic receptor (β2-AR) expression in SACC tissues were evaluated by immunohistochemistry. The NE concentrations in SACC tissues and dorsal root ganglia (DRG) coculture models were measured by ELISA. β2-AR expression in SACC cells was detected by performing quantitative real-time polymerase chain reaction (qRT-PCR) and immunofluorescence assay. SACC cells were treated with NE, the nonselective α-AR blocker phentolamine, the β2-AR antagonist ICI118,551, or were transfected with β2-AR small interfering RNA (siRNA). Proliferation was evaluated in methyl thiazolyl tetrazolium assay, and migration was evaluated in Transwell assay and wound-healing assay. PNI was tested through both Transwell assay and a DRG coculture model. The expressions of epithelial–mesenchymal transition (EMT) markers and matrix metalloproteinases (MMPs) were measured by performing qRT-PCR and Western blot assay.

Results: Sympathetic innervation and β2-AR were highly distributed in SACC tissues and correlated positively with PNI (P=0.035 and P=0.003, respectively). The sympathetic neurotransmitter NE was overexpressed in SACC tissues and DRG coculture models. Exogenously added NE promoted proliferation, migration, and PNI of SACC cells via β2-AR activation. NE/β2-AR signaling may promote proliferation, migration, and PNI by inducing EMT and upregulating MMPs. However, β2-AR inhibition with either an antagonist or siRNA abrogated NE-induced PNI.

Conclusion: Collectively, our findings reveal the supportive role of sympathetic innervation in the pathogenesis of SACC PNI and suggest β2-AR as a potential therapeutic target for treating PNI in SACC.

Keywords: salivary adenoid cystic carcinoma, perineural invasion, sympathetic innervation, β2-adrenergic receptor, norepinephrine

Introduction

Salivary adenoid cystic carcinoma (SACC) is a rare variant of adenocarcinoma that most often originates from the salivary glands and accounts for ~22% of all salivary gland malignancies.[1–3] SACC is well known to researchers for its unique characteristics, including indolent but continuous growth, a high incidence of pulmonary metastasis, potential local recurrence, and perineural invasion (PNI).[4,5] PNI is defined as tumor

cell invasion of nerve fibers and further metastasis to distant sites along the nerve, representing a specific phenomenon resulting from reciprocal interactions between tumor cells and nerves.[6,7] Apart from SACC, PNI has also been widely reported in pancreatic cancer, prostate cancer, gastrointestinal cancer, and head and neck cancer.[7,8] Previously, we performed a meta-analysis of PNI in head and neck adenoid cystic carcinoma, and we found that the PNI incidence of adenoid cystic carcinoma was up to 43.2%. Furthermore, our meta-analysis demonstrated that PNI was an independent prognostic characteristic in head and neck adenoid cystic carcinoma.[9] Currently, surgery (in some cases accompanied by adjuvant radiotherapy) is the primary therapeutic strategy for patients with SACC, and PNI has been widely reported to correlate with local recurrence and poor prognosis for patients with SACC.[1,10] However, there is still no effective therapeutic strategy for treating PNI due to the poor understanding of PNI pathogenesis in SACC.

Although the PNI phenomenon was first reported more than a century ago, a clear understanding of PNI pathogenesis has not been attained. At first, researchers thought that the perineural space served as a low-resistance environment for tumor cells to spread and survive. However, the hypothesis was proven wrong with the development of modern anatomy.[11,12] Recently, with the development of tumor microenvironment theory, an increasing number of studies have focused on reciprocal interactions between tumor cells and nerves.[11] For example, we have investigated the effects of nerve growth factor and chemokine (C-C motif) ligand 5/C-C chemokine receptor type 5 signaling on PNI in SACC.[13] In addition, data from several recent studies indicated that the sympathetic nervous system may play a key role in tumor progression.[14,15] However, whether sympathetic nerves are associated with PNI in SACC remains unknown.

The sympathetic nervous system is a component of the autonomic nervous system, and it plays vital roles under both normal and pathologic conditions. Sympathetic nerves widely innervate tissues and organs throughout the whole body and act by releasing the neurotransmitter norepinephrine (NE) to activate adrenergic receptors.[14] Sympathetic innervation has been detected in prostate cancer, hepatocellular carcinoma, and lung adenocarcinoma, where it may provide survival signals to cells in the tumor microenvironment and contribute to growth, invasion, and metastasis.[15–17] In addition, data from a series of preclinical and epidemiologic studies indicated that β2-adrenergic receptor (β2-AR) blockers may be potential adjuvant therapies for treating malignancies.[18–20] Moreover, a recent study introduced the possibility that NE promotes PNI in pancreatic cancer by activating STAT3 signaling.[21] However, whether sympathetic signaling could regulate malignant biologic behavior including PNI in SACC has, to the best of our knowledge, not been examined to date. Given the important role of sympathetic nerves in regulating tumor progression and its rich innervation in normal salivary gland (NSG) tissues,[22] we hypothesized that sympathetic innervation is positively correlated with SACC PNI and that the sympathetic neurotransmitter NE contributes to PNI in SACC via β2-AR.

To test our hypothesis, we first investigated sympathetic innervation, β2-AR expression, and NE production in SACC tissues and analyzed their correlations with PNI. In addition, we evaluated the proliferation, migration, and PNI abilities of SACC cells treated with NE and the role of β2-AR in mediating NE-induced PNI. Moreover, we further explored the possible mechanism underlying NE-induced PNI and our data suggested β2-AR as a potential therapeutic target for treating PNI in SACC.

Materials and methods

Patient and tissues

A total of 55 surgically resected SACC tissues and 28 NSG tissues were collected from the Department of Oral and Maxillofacial Surgery, School of Stomatology, the Fourth Military Medical University (Xi'an, China) between December 2006 and June 2017. To be enrolled in the study cohort, patients with SACC had to meet the following inclusion criteria: 1) SACCs were histopathologically confirmed by experienced pathologists; 2) SACCs were primary tumors rather than metastasis from other organs. The exclusion criteria were 1) patients who had previously received chemotherapy, radiotherapy, or other cancer-related treatments; 2) patients with incomplete clinical or pathologic data. The present study was approved by the ethics committee of the School of Stomatology, the Fourth Military Medical University. Formal informed consent was not required for the present study because there is no direct contact with the patients, and we did not have to use personal data of the patients. All samples were anonymized.

Reagents and antibodies

Anti-tyrosine hydroxylase (TH) was purchased from Santa Cruz Biotechnology (Santa Cruz, CA, USA). Anti-β2-AR, anti-MMP2, anti-MMP9, anti-GAPDH (glyceraldehyde 3-phosphate dehydrogenase) antibodies, and β2-AR antagonist ICI118,551 were purchased from Abcam (Cambridge, UK). Anti-α1B-AR and anti-α2A-AR antibodies were

purchased from Proteintech Group (Wuhan, China). Anti-Slug antibody was purchased from Cell Signaling Technology (Danvers, MA, USA). Anti-E-cadherin, anti-β1-AR, anti-vimentin antibodies, and rabbit IgG isotype control were purchased from GeneTex (San Antonio, TX, USA). Adrenergic receptor agonist NE was purchased from Aladdin (Shanghai, China). Nonselective α-AR blocker phentolamine hydrochloride was purchased from Sigma-Aldrich (Saint Louis, MO, USA).

Cell lines and culture conditions

The human SACC cell lines SACC-83 and SACC-LM were kindly provided by Dr Shenglin Li (Peking University, China). Use of the SACC cell lines was approved by the ethics committee of the School of Stomatology (The Fourth Military Medical University). Both cell lines were cultured in RPMI-1640 medium (Hyclone, Logan, UT, USA) supplemented with 10% FBS (Gibco, Carlsbad, CA, USA), 100 U/mL penicillin, and 0.1 mg/mL streptomycin (Hyclone) at 37°C in 5% CO_2.

Immunohistochemistry (IHC)

Tumor sections were first stained with H&E to confirm the presence of PNI (Figure S1). PNI was defined as described previously.[6] The IHC assay was performed using the streptavidin–biotin–peroxidase method, as we have previously described.[13] Briefly, 5-μm-thick sections were cut from formalin-fixed, paraffin-embedded tissue specimens. Then, the sections were deparaffinized in xylene and rehydrated using a graded series of alcohol solutions. Epitope retrieval was performed by placing the sections in boiling citrate buffer (pH 6.0) for 5 minutes. Endogenous peroxidase activity was blocked with 3% hydrogen peroxide solution for 20 minutes. Subsequently, the slides were incubated with 3% normal goat serum (ZSGB-BIO Ltd., China) at 37°C for 40 minutes to block nonspecific staining. Then, the slides were incubated overnight with primary antibodies against TH (1:1,000) or β2-AR (1:1,000) at 4°C. Subsequently, the slides were washed and analyzed using the Biotinylated-Streptavidin HRP Detection System (ZSGB-BIO, Ltd.). Finally, the DAB Horseradish Peroxidase Color Development Kit (ZSGB-BIO, Ltd.) was used to visualize immunoreactivity. Tissue slides were then counterstained with hematoxylin (ZSGB-BIO Ltd.), dehydrated, and mounted. Sections incubated with PBS were used as negative controls.

Two experienced pathologists evaluated the IHC staining in a blinded manner, without knowledge of the clinicopathologic data of the SACC patients. They observed all tissue slides carefully under a light microscope (4N75; Nikon, Tokyo, Japan) to identify positive sympathetic innervation or β2-AR expression. Then, positively stained slides were selected for further quantitative analysis, as reported previously.[5,15,23] For sympathetic innervation, the slides were first observed at low magnification (40×), to locate "hot spots", that is, regions containing the highest density of positive sympathetic nerve fibers. Then, 3–5 high-magnification (100×) microscopic fields were randomly chosen from the "hot spots" to estimate the positive nerve areas. The positive nerve areas of each field were measured and calculated using Image-Pro Plus v6.0 software (Media Cybernetics, Inc., Bethesda, MD, USA). In contrast, the β2-AR expression levels were estimated based on the integrated optical density (IOD), which was measured using Image-Pro Plus v6.0 software. Similar to the measurement process used to study sympathetic innervation, 3–5 high-magnification (100×) microscopic fields were randomly chosen from "hot spots" found at a low magnification (40×) to estimate the IOD value. The mean IOD value for each field was calculated using the following formula: mean IOD = IOD of positive cells/total areas of the field.[23] Finally, we compared the positive sympathetic nerve areas and β2-AR expression levels, according to the positive nerve areas and mean IODs from three to five randomly chosen fields, respectively.

ELISA experiments

NE levels in SACC tissues, NSG tissues, and culture supernatant from dorsal root ganglia (DRG) coculture models were determined using an ELISA Kit (Westang, Shanghai, China), according to the manufacturer's protocols.

Quantitative real-time polymerase chain reaction (qRT-PCR)

Total RNA was extracted from cells using TRNzol reagent (TIANGEN Biotechnology, Beijing, China) and converted into cDNA using a First-Strand Synthesis Kit (TIANGEN Biotechnology). PCR amplifications were performed with the SuperReal PreMix Plus (SYBR green) (TIANGEN Biotechnology) on a BIO-Rad system. The results were expressed as the copy number of each gene relative to that of GAPDH. The relative expressions of genes were calculated by the $2^{-\Delta\Delta Ct}$ method.[24] Sequences of primers for each gene are listed in Table 1.

Immunofluorescence

Immunofluorescence was performed to evaluate α1B-AR, α2A-AR, β1-AR, and β2-AR expression in SACC-83 and

Table 1 The primers used in the study

Gene	Sequence (5′–3′)	
	Upper	**Lower**
GAPDH	CTCCTCCACCTTTGACGCTG	TCCTCTTGTGCTCTTGCTGG
E-cadherin	TGTCGTCACCACAAATCCAGT	CCAGGGGACAAGGGTATGAAC
N-cadherin	AGGCTTCTGGTGAAATCGCA	AAATCTGCAGGCTCACTGCT
Vimentin	GGACCAGCTAACCAACGACA	AAGGTCAAGACGTGCCAGAG
Slug	GCTACCCAATGGCCTCTCTC	CTTCAATGGCATGGGGGTCT
MMP2	CCAGATCGCGAGAGAGCAATA	GTAGTTGGCCACATCTGGGT
MMP9	CCTGGGCAGATTCCAAACCT	GTACACGCGAGTGAAGGTGA
α1A-AR	CGGGGAGGAAGTCTAGGACA	GTCTACCACCCACCCCATTC
α1B-AR	GAAGAAGACCACGGGGGAAG	TCTTAGAGTCCGCCCTCCAT
α1D-AR	GCCTACGAATTGGCCGACTA	AGCTGCCCTGATCAGTTTCC
α2A-AR	ATCCTGGCCTTGGGAGAGAT	TCTCAAAGCAGGTCCGTGTC
α2B-AR	TATCGGCCTTCCCTTGGAGA	CTCGGTGCCCTTCCAAATCT
α2C-AR	TCTGGATCGGCTACTGCAAC	CTCCGTCGGAAGAGGATGTG
β1-AR	TCCTTGTGTAGGGCAAACCC	CGCCTGGTCCTTCCAACTAA
β2-AR	TGCTATGCCAATGAGACCTG	TCCACCTGGCTAAGGTTCTG
β3-AR	TACTCTGCGCTGGCTTTTGA	AAAGGCTCAAGCTCACTCCC

Abbreviations: AR, adrenergic receptor; GAPDH, glyceraldehyde 3-phosphate dehydrogenase; MMP, matrix metalloproteinase.

SACC-LM cells. The cells were cultured on coverslips in a six-well plate for 24 hours at 37°C in a cell incubator. Then the coverslips were fixed in 4% paraformaldehyde for 15 minutes after washing with PBS. To block nonspecific reactions, the coverslips were incubated with normal goat serum at room temperature for 40 minutes. Then, the coverslips were incubated for 16 hours at 4°C in a humidified chamber with α1B-AR (1:200), α2A-AR (1:200), β1-AR (1:200), and β2-AR antibody (1:200). PBS and rabbit IgG isotype control were used as negative controls. After washing with PBS, the coverslips were incubated with secondary antibody (Alexa-488 goat anti rabbit; 1:200, Yeasen Ltd, Shanghai, China) at 37°C for 15 minutes and DAPI was used as a counterstain. Finally, the slides were examined under an Olympus microscope. Then, positively stained slides were selected for further quantitative analysis, and 3–5 high-magnification (400×) microscopic fields were randomly chosen from a slide to estimate the fluorescence intensity. The fluorescence microscope fields were assessed using Image-Pro Plus v6.0 software (Media Cybernetics, Inc., Bethesda, MD, USA), and the mean density (IOD/area) of each image was collected.

siRNA transfection

Sequences of small interfering RNA (siRNA) used for knockdown of β2-AR were designed and obtained from GenePharma (Shanghai, China). The sequences were listed as follows: β2-AR siRNA, 5′-CCUAGCGAUAACAUU GAUUTT-3′, and control siRNA, 5′-UUCUCCGAACGUG UCACGUTT-3′. SACC cells were transfected with β2-AR siRNA or control siRNA using Lipofectamine 2000 (Invitrogen, Carlsbad, CA, USA), according to the manufacturer's protocol. The knockdown efficiency was determined at both the mRNA and protein levels.

MTT assay

The effects of NE, ICI118,551, and phentolamine on the proliferation of SACC cell lines were tested by MTT assay. The SACC-83 and SACC-LM cells were seeded in 200 μL complete medium in 96-well plates with an initial cell density of 2×10^3/well. After serum starving for 24 hours, the medium was removed, NE, ICI118,551, phentolamine, or their combination in 1% serum medium was added to the culture plates. After an incubation of 48 hours, the medium was removed and MTT reagent (5 mg/mL) was added and incubation was continued for an additional 4 hours. Then, 150 μL of dimethyl sulfoxide (Sigma-Aldrich, St Louis, MO, USA) was added, and the OD was measured at 490 nm using an ELISA plate reader. The cells cultured in 1% serum medium served as the control group. The relative growth rate was calculated according to the following formula: experimental OD value/control OD value. All experiments were performed in triplicate.

Transwell migration assay and wound-healing assay

For the Transwell migration assay, 8 μm pores (BD Biosciences, Franklin Lakes, NJ, USA) were used in 24-well plates to evaluate migration ability. SACC cells were serum

starved overnight and 1×10^5 cells were added onto the upper inserts in 200 µL serum-free RPMI 1640 media. The lower chamber was added with 600 µL 1% serum media as a chemoattractant. The inserts were removed after 24 hours and nonmigrating cells on the upper surface of the inserts were wiped with a cotton swab. Migrated cells on the undersurface of the membrane were fixed in 4% paraformaldehyde for 10 minutes and then stained with crystal violet staining solution (Beyotime, Shanghai, China) for 10 minutes. Quantification was performed by counting the migrated cells in five randomly selected high-power fields (200×).

For wound-healing assay, cells were grown on six-well plates to about 80% confluence. A scratch was generated with a 200 µL pipette tip. Subsequently, the wounded monolayers were washed with PBS three times to remove nonadherent cells, and then 2 mL culture medium with 1% serum was added with the indicated agents for 36 hours. Wound healing was quantified and photographed. The wound-healing assay was performed in triplicate.

Transwell PNI assay

The promoting effects of NE on PNI activities of SACC-83 and SACC-LM cells were investigated by both Transwell PNI assay and DRG coculture model. For the Transwell PNI assay, 8 µm pores (BD Biosciences, Franklin Lakes, NJ, USA) were used in 24-well plates to evaluate PNI ability. SACC cells were serum starved overnight and 1×10^5 cells were added onto the Matrigel (BD Biosciences, Franklin Lakes, NJ, USA)-covered inserts in 200 µL serum-free RPMI 1640 media. The lower chamber was seeded with two DRG explants from a newborn Sprague-Dawley rat in 600 µL 1% serum media to simulate the perineural surrounding environment. The inserts were removed after 24 hours and noninvaded cells on the upper surface of the inserts were wiped with a cotton swab. Invaded cells on the undersurface of the membrane were fixed in 4% paraformaldehyde for 10 minutes and then stained with crystal violet staining solution (Beyotime, Shanghai, China) for 10 minutes. Quantification was performed by counting the invaded cells in five randomly selected high-power fields (200×).

DRG coculture model

The in vitro DRG coculture model of PNI was based on a technique originally described in a prostate cancer study.[25] Briefly, we plated a colony of ~5×10^4 serum-starved SACC cells in a 12-well plate with 20 µL Matrigel. Then, the 12-well plate was incubated at 37°C to solidify the Matrigel. Thereafter, an excised DRG from a newborn Sprague-Dawley rat was transferred into the center of a 10 µL drop of Matrigel, ~1 mm adjacent to the colony of SACC cells. SACC cells and DRGs were cultured in 1% serum media at 37°C and 5% CO_2. At 72 hours after the cancer cells were added, the plates were examined using an Axiovert 200 M microscope (Carl Zeiss, German), and images were acquired using a Photometrics Coolsnap ES camera (Photometrics, Tucson, AZ, USA). Quantification was performed by calculating the nerve invasion index and the DRG outgrowth index at 72 hours relative to that at 24 hours.[26,27] The total distance between the edge of the DRG and the edge of the cancer cell colony was defined as γ. The distance that the cancer cell colony migrated toward the DRG was defined as α, and the outgrowth distance of the DRG toward the cancer cell colony was defined as β. The nerve invasion index was calculated as α/γ, and the DRG outgrowth index was calculated as β/γ.

Western blot

Cell protein extracts were collected using radioimmunoprecipitation buffer (Applygen Technologies, Inc., Beijing, China). Protein concentration was determined by BCA Protein Assay Kit (Applygen Technologies, Inc., Beijing, China). The protein extracts were mixed with 5× loading buffer (Beyotime, Shanghai, China) and boiled for 5 minutes. Protein extracted from each sample was separated by 10% SDS-PAGE and were transferred onto polyvinylidene difluoride membranes (Millipore, Temecula, CA, USA). The membranes were blocked in 5% nonfat dry milk for 1 hour and incubated overnight at 4°C with primary antibodies. Then, the membranes were incubated with horseradish peroxidase-conjugated secondary antibody (ZSGB-BIO Ltd.) for 2 hours. The membranes were scanned by ChemidocTM XRS + with Image LabTM software (Bio-Rad Laboratories, Inc., Hercules, CA, USA) and semiquantitative analysis was performed using the Image LabTM software.

Statistical analysis

Statistical analysis was carried out using SPSS software (version 19.0, IBM, USA) and GraphPad Prism (version 6.01, GraphPad Software, Inc., La Jolla, CA, USA). The association of sympathetic innervation or β2-AR expression with clinicopathologic characteristics was analyzed using Pearson's chi-squared test or Fisher's exact test. The logistic regression analysis was used to analyze the clinicopathologic characteristics that were independently associated with PNI. The Student's *t*-test or Mann–Whitney U-test was used to compare the means of two groups. $P<0.05$ was considered as the threshold for significance in all analyses.

Results

Sympathetic innervation positively correlated with PNI in patients with SACC

To evaluate the association of sympathetic innervation with PNI in SACC tissues, we retrospectively analyzed sympathetic nerve areas from 55 SACC tissues. IHC results demonstrated that positive sympathetic innervation occurred in both tumor parenchyma and stroma (Figure 1). In SACC tissues positive for sympathetic innervation with PNI, gross sympathetic nerve fibers were distributed in tumor parenchyma, and tumor cells had invaded and spread along the sympathetic nerve fibers (Figure 1A). In SACC tissues positive for sympathetic innervation, but without PNI, fine sympathetic nerve fibers were mainly distributed in the tumor stroma (Figure 1B).

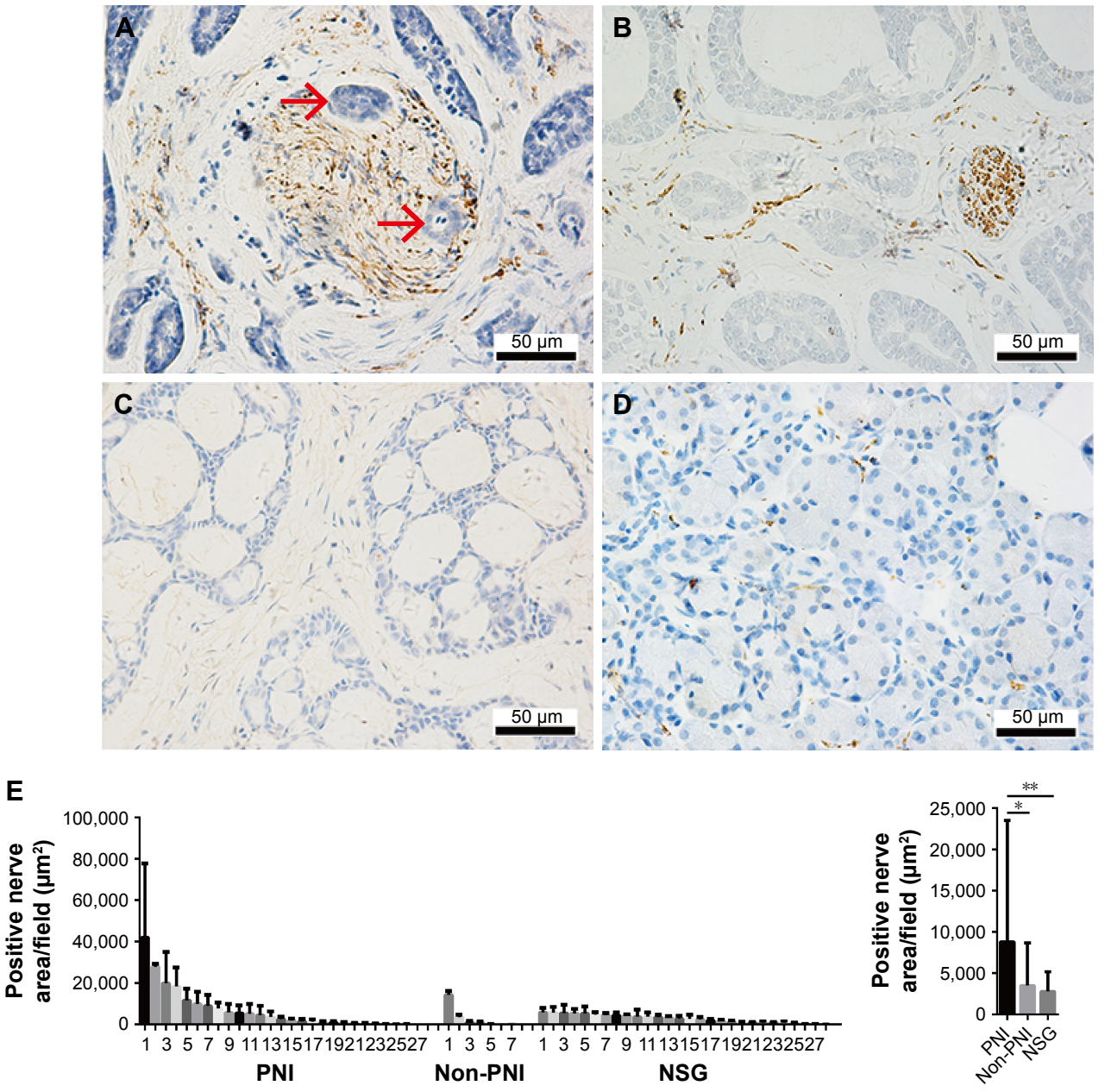

Figure 1 Sympathetic innervation correlated positively with PNI in SACC tissues.

Notes: (**A**) Sympathetic nerve fibers were invaded by tumor cells in SACC tissues with PNI (invaded tumor cells are indicated with red arrowheads). (**B**) Fine sympathetic nerve fibers were mainly distributed in the stroma of SACC tissues without PNI. (**C**) Negative sympathetic innervation in SACC tissues without PNI. (**D**) Tiny sympathetic nerve fibers were sparsely scattered in NSG tissues. (**E**) Quantitative comparison of the sympathetic innervation areas in SACC tissues with PNI, SACC tissues without PNI, and NSG tissues. Left, quantification of sympathetic innervation areas in PNI SACC tissues (n=27), non-PNI SACC tissues (n=7), and NSG tissues (n=28). Each bar represents the average sympathetic innervation areas of three to five fields obtained from SACC or NSG tissue. Right, average sympathetic innervation areas in PNI SACC tissues, non-PNI SACC tissues, and NSG tissues. Original magnification, 400×; scale bar =50 μm. *$P<0.05$, **$P<0.01$. The error bars indicate the SD.

Abbreviations: NSG, normal salivary gland; PNI, perineural invasion; SACC, salivary adenoid cystic carcinoma.

In SACC tissues negative for sympathetic innervation without PNI, no sympathetic nerve fibers were distributed in the tumor tissues (Figure 1C). In addition, although sympathetic innervation was detected in all 28 NSG tissues, tiny sympathetic nerve fibers were sparsely scattered in the glandular stroma (Figure 1D). Quantitative analysis suggested that the positive sympathetic nerve areas in SACC tissues with PNI were significantly larger than in the SACC tissues without PNI (Figure 1E, $P<0.05$), while the sympathetic nerve areas in NSG tissues were the smallest among the three groups.

We also analyzed the correlation between sympathetic innervation and the clinicopathologic characteristics. Among the 55 SACC tissues studied, 34 (61.8%) were classified as showing positive sympathetic innervation and 21 (38.2%) were negative for sympathetic innervation (Table 2). Statistical analysis showed that sympathetic innervation correlated with PNI ($P=0.035$) and the M category ($P=0.010$), while no correlation was found for other clinicopathologic characteristics, including the N category. Such a correlation was also consistent with the high pulmonary metastasis and low lymphatic metastasis characteristics of SACC. Furthermore, the positive association between sympathetic innervation and PNI was further confirmed by univariate and multivariate logistic regression analyses (Table 3, $P=0.002$ and $P=0.042$).

Table 2 Correlation of sympathetic innervation and β2-AR expression with the clinicopathologic characteristics of SACC

Variables	Total (N=55) N (%)	Sympathetic innervation		*P*-value	β2-AR expression		*P*-value
		Yes (N=34) N (%)	None (N=21) N (%)		Yes (N=38) N (%)	None (N=17) N (%)	
Gender				0.821			0.057
Male	22 (40.0)	14 (63.6)	8 (36.4)		12 (54.5)	10 (45.5)	
Female	33 (60.0)	20 (60.6)	13 (39.4)		26 (78.8)	7 (21.2)	
Age, years				0.357			0.751
≤40	7 (12.7)	6 (85.7)	1 (14.3)		5 (71.4)	2 (28.6)	
40–55	25 (45.5)	14 (56.0)	11 (44.0)		16 (64.0)	9 (36.0)	
≥55	23 (41.8)	14 (60.9)	9 (39.1)		17 (73.9)	6 (26.1)	
Site				0.219			0.156
MiSG	27 (49.1)	14 (51.9)	13 (48.1)		18 (66.7)	9 (33.3)	
MaSG	21 (38.2)	16 (76.2)	5 (23.8)		17 (81.0)	4 (19.0)	
Other	7 (12.7)	4 (57.1)	3 (42.9)		3 (42.9)	4 (57.1)	
TNM stage				0.927			0.035*
I–II	24 (43.6)	15 (62.5)	9 (37.5)		13 (54.2)	11 (45.8)	
III–IV	31 (56.4)	19 (61.3)	12 (38.7)		25 (80.6)	6 (19.4)	
T category				0.606			0.083
1–2	26 (47.3)	17 (65.4)	9 (34.6)		15 (57.7)	11 (42.3)	
3–4	29 (52.7)	17 (58.6)	12 (41.4)		23 (79.3)	6 (20.7)	
N category				0.573			0.165
0	51 (92.7)	31 (60.8)	20 (39.2)		34 (66.7)	17 (33.3)	
1–2	4 (7.3)	3 (75.0)	1 (25.0)		4 (100.0)	0 (0)	
M category				0.010*			0.166
0	42 (76.4)	22 (52.4)	20 (47.6)		27 (64.3)	15 (35.7)	
1	13 (23.6)	12 (92.3)	1 (7.7)		11 (84.6)	2 (15.4)	
PNI				0.035*			0.003*
Yes	38 (69.1)	27 (71.1)	11 (28.9)		31 (81.6)	7 (18.4)	
None	17 (30.9)	7 (41.2)	10 (58.8)		7 (41.2)	10 (58.8)	
Histologic subtype				0.299			0.791
Cribriform/tubular	51 (92.7)	33 (64.7)	18 (35.3)		35 (68.6)	16 (31.4)	
Solid	4 (7.3)	1 (25.0)	3 (75.0)		3 (75.0)	1 (25.0)	
Chemotherapy				0.258			0.365
Yes	21 (38.2)	11 (52.4)	10 (47.6)		13 (61.9)	8 (38.1)	
None	34 (61.8)	23 (67.6)	11 (32.4)		25 (73.5)	9 (26.5)	
Radiotherapy				0.157			0.812
Yes	40 (72.7)	27 (67.5)	13 (32.5)		28 (70.0)	12 (30.0)	
None	15 (27.3)	7 (46.7)	8 (53.3)		10 (66.7)	5 (33.3)	
Recurrence				0.762			0.990
Yes	13 (23.6)	9 (69.2)	4 (30.8)		9 (69.2)	4 (30.8)	
None	42 (76.4)	25 (59.5)	17 (40.5)		29 (69.0)	13 (31.0)	

Note: *Mean $P<0.05$.

Abbreviations: β2-AR, β2-adrenergic receptor; MaSG, major salivary gland; MiSG, minor salivary gland; PNI, perineural invasion; SACC, salivary adenoid cystic carcinoma.

Table 3 Univariate and multivariate logistic regression analyses of the clinicopathologic characteristics associated with PNI in SACC

Variables	Univariate analysis		Multivariate analysis	
	HR (95% CI)	*P*-value	HR (95% CI)	*P*-value
M	7.385 (0.875–62.323)	0.046*	4.062 (0.398–41.418)	0.237
Sympathetic innervation	7.733 (2.142–27.915)	0.002*	3.846 (0.935–15.826)	0.042*
β2-AR	6.327 (1.782–22.463)	0.004*	3.583 (0.874–14.684)	0.076

Note: *Mean $P<0.05$.
Abbreviations: β2-AR, β2-adrenergic receptor; PNI, perineural invasion; SACC, salivary adenoid cystic carcinoma.

β2-AR overexpression positively correlated with PNI in patients with SACC

To elucidate the biologic significance of β2-AR overexpression in SACC with PNI, we measured β2-AR expression in 55 SACC tissues by IHC. β2-AR expression occurred predominantly on the cellular membrane and in the cytoplasm of tumor cells, and β2-AR was highly expressed in SACC with PNI compared to SACC without PNI (Figure 2A and B). In addition, strongly positive β2-AR expression was also detected in nerve fibers invaded by SACC cells, and β2-AR was mainly expressed on the membrane and cytoplasm in neural cells (Figure 2A). β2-AR was not expressed in SACC tissues without PNI (Figure 2C). In contrast, β2-AR was only expressed on the cellular membrane of salivary ducts in NSG tissues (Figure 2D). Quantitative analysis revealed that β2-AR overexpression occurred in SACC tissues with PNI, in contrast to both SACC without PNI (Figure 2E, $P>0.05$) and NSG tissues (Figure 2E, $P<0.05$).

We further examined the correlation between β2-AR expression and clinicopathologic characteristics in SACC (Table 2). Among the 55 SACC patients, 38 (69.1%) were positive for β2-AR expression, and 17 (30.9%) were negative for β2-AR expression. As shown in Table 2, positive β2-AR expression in patients with SACC positively correlated with the TNM stage ($P=0.035$) and PNI ($P=0.003$), whereas no correlation was found for other clinicopathologic prognostic variables. Moreover, a positive association between β2-AR overexpression and PNI was confirmed by univariate and multivariate logistic regression analyses (Table 3, $P=0.004$ and $P=0.076$, respectively).

NE was highly expressed in both SACC tissues with PNI and DRG coculture models of PNI

An ELISA-based method was performed to investigate whether NE was expressed in SACC tissues and the supernatant of DRG coculture models of PNI. NE was detected in both SACC and NSG tissues (Figure 3A), and quantitative analysis revealed that the average NE concentration in SACC with PNI increased significantly vs SACC without PNI or NSG (Figure 3B, $P<0.01$ and $P<0.001$, respectively). Next, we evaluated the NE concentration in the supernatant of a DRG cocultured with SACC-LM, a DRG cocultured with SACC-83, SACC-LM, SACC-83, DRG, and pure culture medium as a control group. The supernatant of a DRG cocultured with SACC-LM showed the highest NE concentration among the six groups, followed by the supernatant of a DRG cocultured with SACC-83 (Figure 3C). Moreover, we found that NE levels were significantly elevated in the supernatants of SACC-LM and SACC-83 cells, compared to the control group (Figure 3C, $P<0.001$ and $P<0.001$, respectively). In addition, NE was also detected in the supernatant of a DRG (Figure 3C).

β2-AR was overexpressed in SACC cell lines

NE plays a regulatory role by activating α-ARs and β-ARs. α-ARs are composed of six subtypes (α1A-AR, α1B-AR, α1D-AR, α2A-AR, α2B-AR, and α2C-AR) and β-ARs are composed of three subtypes (β1-AR, β2-AR, and β3-AR). Therefore, we investigated the expression levels of α-AR subtypes and β-AR subtypes in the SACC-83 and SACC-LM cell lines by qRT-PCR. We found that the expression levels of α1B-AR, α2A-AR, β1-AR, and β2-AR were relatively high in both SACC cell lines, among which β2-AR was predominantly expressed in both SACC cell lines (Figure 4A and B). Moreover, α1B-AR, α2A-AR, β1-AR, and β2-AR expressions were verified by immunofluorescence in SACC-83 and SACC-LM cells (Figure 4C; see Figure S2 for negative controls). Quantitative analysis of immunofluorescence results confirmed that β2-AR was predominantly expressed in both SACC cell lines (Figure 4D and E).

NE contributed to SACC cell proliferation and migration via β2-AR

To explore the effects of NE, ICI118,551, and phentolamine on SACC cell viability and migration, we treated SACC-83 and SACC-LM cells with different concentrations of NE

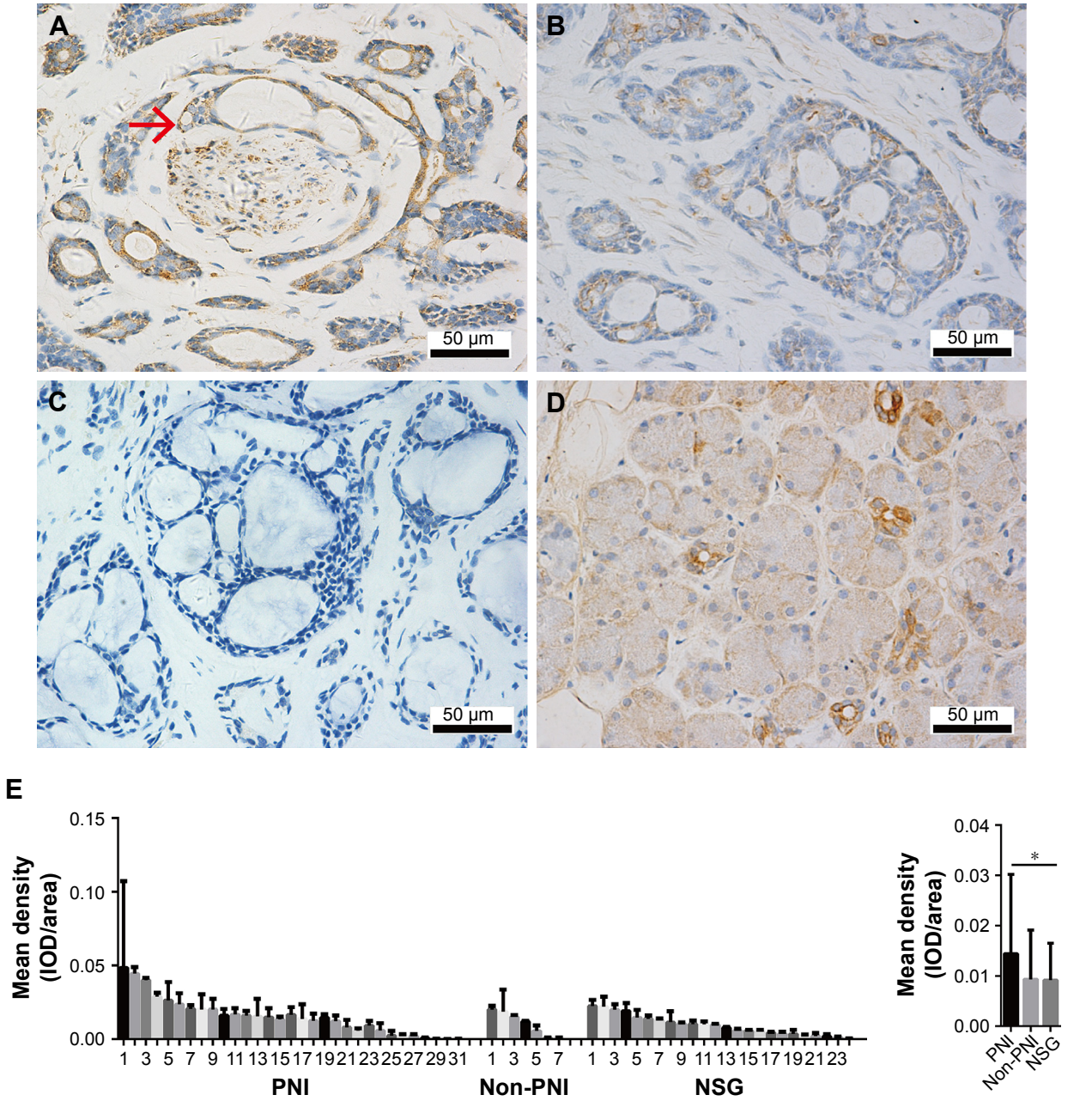

Figure 2 β2-AR expression correlated positively with PNI in SACC tissues.

Notes: (**A**) β2-AR was strongly expressed in both nerve fibers and adjacent tumor cell membranes in SACC tissues with PNI (invaded tumor cells are indicated by red arrowheads). (**B**) β2-AR was weakly expressed in SACC tissues without PNI. (**C**) Negative β2-AR expression in SACC tissues without PNI. (**D**) β2-AR was mainly expressed on the cellular membranes of salivary ducts in NSG tissues. (**E**) Quantitative comparison of the mean density (IOD/area) of β2-AR expression in PNI SACC tissues, non-PNI SACC tissues, and NSG tissues. Left, quantification of β2-AR-expressing mean density in PNI SACC tissues (n=31), non-PNI SACC tissues (n=7), and NSG tissues (n=24). Each bar represents the mean density of β2-AR expression observed in three to five fields obtained from SACC or NSG tissue. Right, mean β2-AR expression densities in PNI SACC tissues, non-PNI SACC tissues, and NSG tissues. Original magnification, 400×; scale bar =50 μm. *$P<0.05$. The error bars indicate the SD.

Abbreviations: β2-AR, β2-adrenergic receptor; IOD, integrated optical density; NSG, normal salivary gland; PNI, perineural invasion; SACC, salivary adenoid cystic carcinoma.

(0.1–100 μM), ICI118,551 (0.1–100 μM), and phentolamine (0.1–50 μM) for 48 hours (Figure 5; see Figures S3 and S5 for phentolamine). NE promoted SACC-83 and SACC-LM cell proliferation in a concentration-dependent manner, and the viability of SACC cells peaked at an NE concentration of 10 μM (Figure 5A and B). In contrast, ICI118,551 inhibited the viability of SACC-83 and SACC-LM cells in a concentration-dependent manner (Figure 5A and B; Figure S4). Furthermore, 10 μM ICI118,551 completely abrogated the NE-dependent increase in SACC-83 and SACC-LM cell proliferation, suggesting that β2-AR mediated NE-induced proliferation (Figure 5A and B; Figure S4). However, 50 μM phentolamine

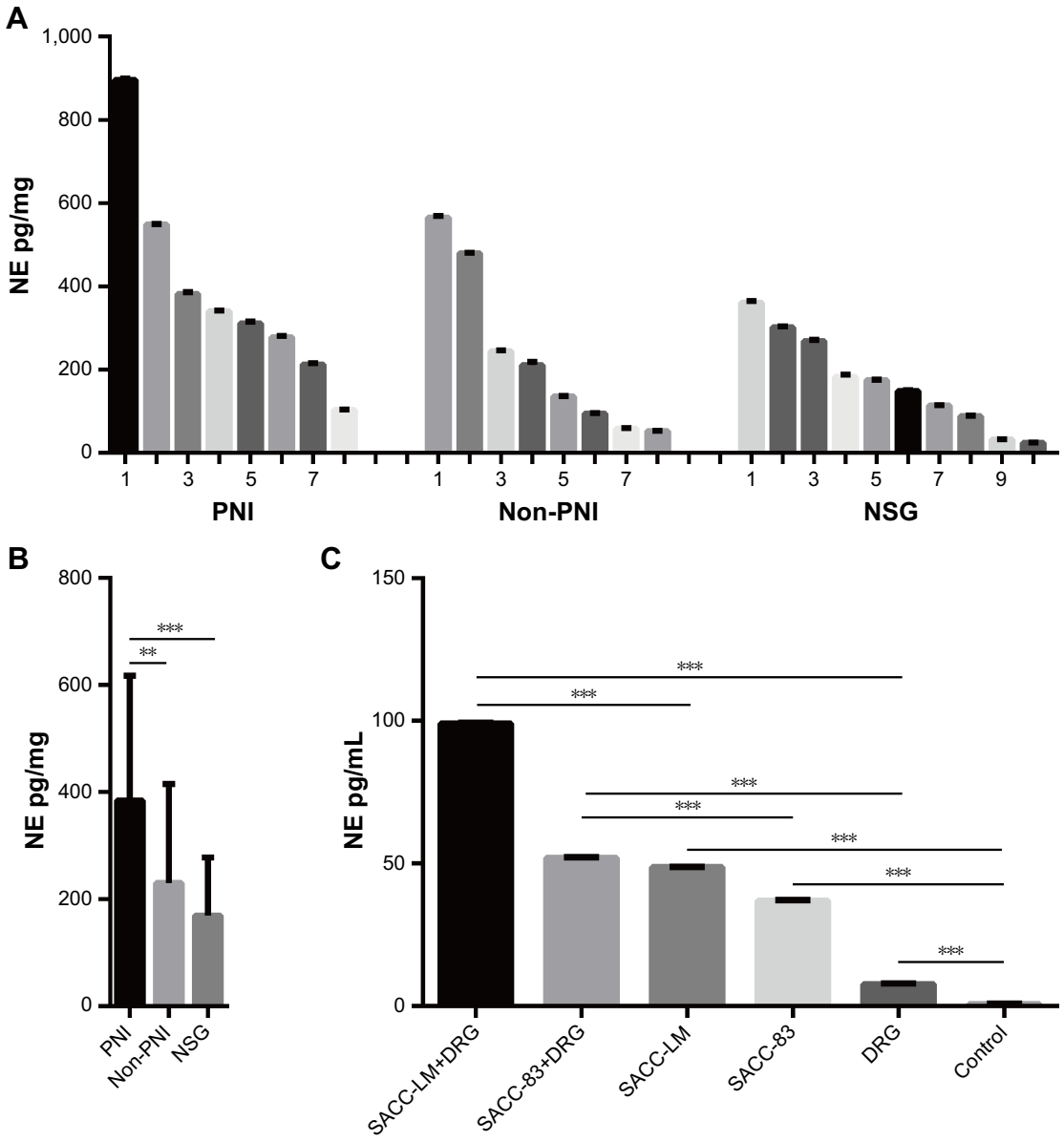

Figure 3 NE was highly expressed in both SACC tissues with PNI and DRG coculture models of PNI.
Notes: (**A**) Quantitative comparison of NE levels in PNI SACC tissues (n=8), non-PNI SACC tissues (n=8), and NSG tissues (n=10). (**B**) Average NE levels in PNI SACC tissues, non-PNI SACC tissues, and NSG tissues. (**C**) Quantitative comparison of NE levels in supernatant of a DRG cocultured with SACC-LM, a DRG cocultured with SACC-83, SACC-LM, and SACC-83, and a DRG and a pure culture medium (as a control group). $^{**}P<0.01$, $^{***}P<0.001$. The error bars indicate the SD.
Abbreviations: DRG, dorsal root ganglia; NE, norepinephrine; NSG, normal salivary gland; PNI, perineural invasion; SACC, salivary adenoid cystic carcinoma.

failed to abrogate the NE-dependent increase in SACC-83 and SACC-LM cell proliferation, suggesting that NE-induced proliferation was not mediated by α-AR (Figure S3B and D). We then investigated whether β2-AR could mediate the effects of NE on SACC-83 and SACC-LM cell migration. Similar to the proliferation assay results, the Transwell migration assay showed that NE promoted SACC cell migration in a concentration-dependent manner and that 10 μM NE showed the greatest effect on migration (Figure 5C). In addition, wound-healing assay confirmed the promotion effect of 10 μM NE on SACC-83 and SACC-LM cell migration, and also demonstrated that 10 μM ICI118,551 markedly inhibited NE-induced SACC cell migration (Figure 5D and E, $P<0.01$ for SACC-83 and $P<0.001$ for SACC-LM, respectively). In contrast, phentolamine did not abrogate the NE-upregulated migration of SACC-83 and SACC-LM cells (Figure S5A and B). These results suggest that NE promoted SACC cell proliferation and migration by activating β2-AR.

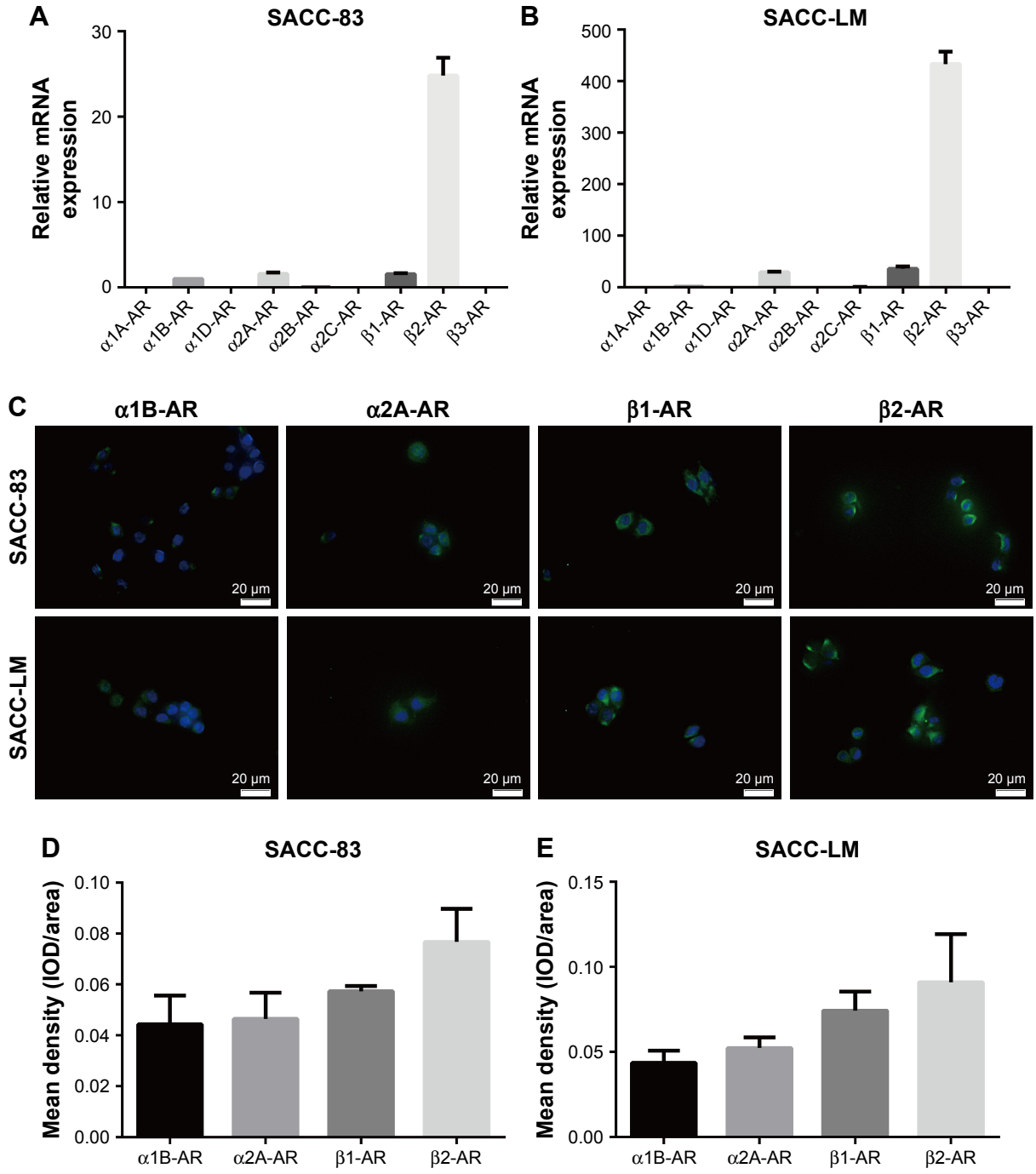

Figure 4 β2-AR was overexpressed in SACC-83 and SACC-LM cell lines.
Notes: (**A**, **B**) qRT-PCR analysis showing α1A-AR, α1B-AR, α1D-AR, α2A-AR, α2B-AR, α2C-AR, β1-AR, β2-AR, and β3-AR mRNA expression levels in SACC-83 and SACC-LM cells. (**C**) Immunofluorescence analysis of α1B-AR, α2A-AR, β1-AR, and β2-AR expression in SACC-83 and SACC-LM cells. (**D**, **E**) Quantitative comparison of the mean density (IOD/area) of α1B-AR, α2A-AR, β1-AR, and β2-AR expression in SACC-83 and SACC-LM cells. Original magnification, 400×; scale bar=20 μm.
Abbreviations: AR, adrenergic receptor; IOD, integrated optical density; qRT-PCR, quantitative real-time polymerase chain reaction; SACC, salivary adenoid cystic carcinoma.

NE contributed to SACC PNI via β2-AR

To explore the effect of NE on PNI by SACC cells, a modified Transwell PNI model was established with DRG explants seeded in the lower chamber. The results showed that the number of invaded cells markedly increased with the addition of 10 μM NE compared to the control (Figure 6A, $P<0.01$ for SACC-83 and $P<0.01$ for SACC-LM, respectively). However, 10 μM ICI118,551 significantly suppressed the invasive ability of SACC cells both in the control (Figure 6A, $P<0.01$ for SACC-83 and $P<0.05$

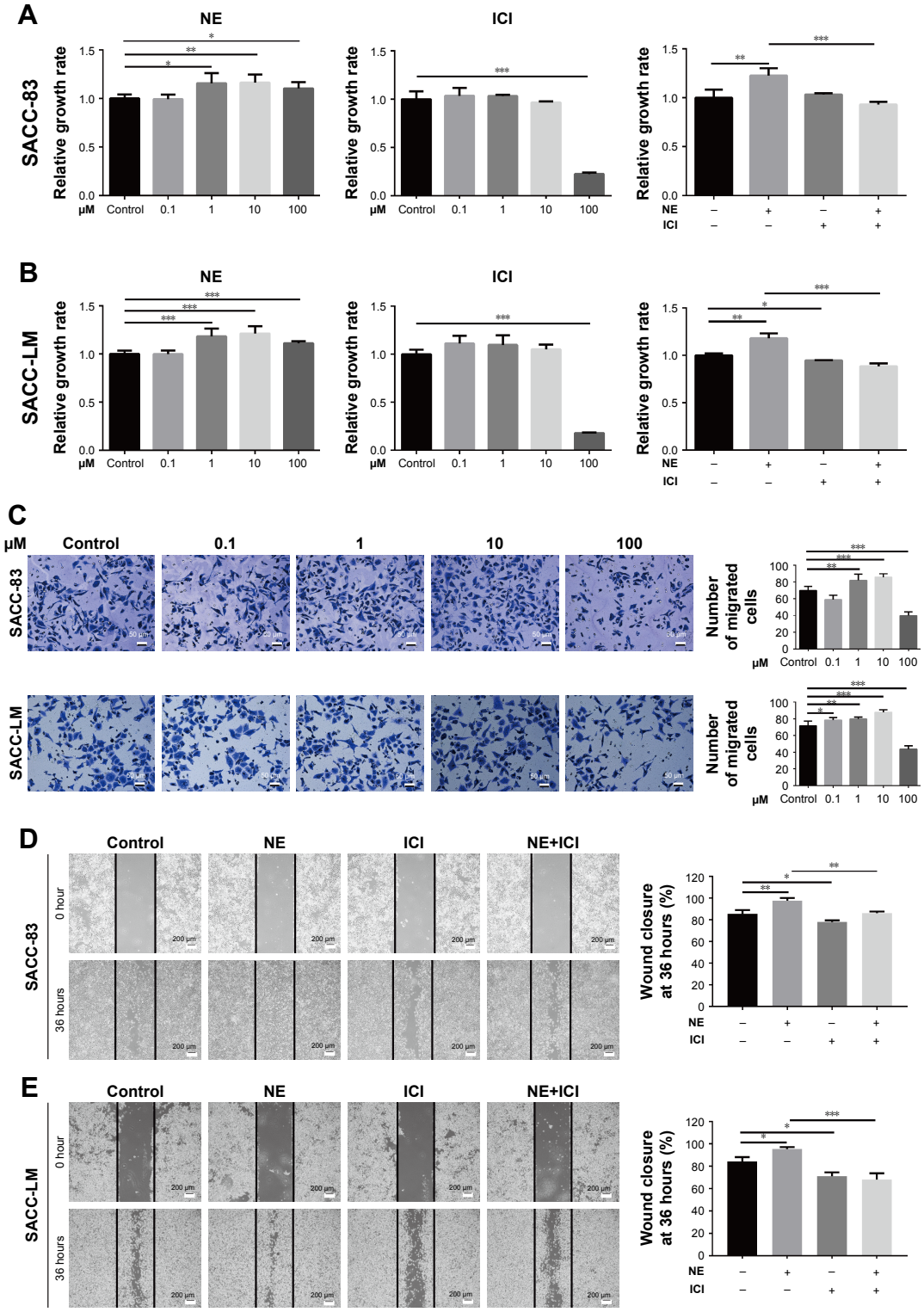

Figure 5 NE contributed to SACC cell proliferation and migration via β2-AR.

Notes: (**A**, **B**) MTT assay showed that incubating SACC-83 and SACC-LM cells with different concentrations of NE (0.1–100 μM) for 48 hours promoted SACC-83 and SACC-LM cell proliferation in a concentration-dependent manner. Treatment with 10 μM NE significantly promoted the proliferation of SACC-83 and SACC-LM cells. ICI118,551 inhibited the proliferation of SACC-83 and SACC-LM cells in a concentration-dependent manner. Treatment with 10 μM ICI118,551 significantly inhibited the NE-induced proliferation of SACC-83 and SACC-LM cells. (**C**) Transwell migration assay showed that NE promoted SACC-83 and SACC-LM cell migration in a concentration-dependent manner. Treatment with 10 μM NE significantly promoted SACC-83 and SACC-LM cell migration. The number of migrated cells was quantified. Original magnification, 200×; scale bar =50 μm. (**D, E**) Wound-healing assay comparing the migration abilities of SACC-83 and SACC-LM cells treated with 10 μM NE and/or 10 μM ICI118,551. The wound-closure percentage was quantified at 36 hours after scratching relative to that at 0 hour. Original magnification, 40×; scale bar =200 μm. **P*<0.05, ***P*<0.01, ****P*<0.001. The error bars indicate the SD.

Abbreviations: β2-AR, β2-adrenergic receptor; NE, norepinephrine; SACC, salivary adenoid cystic carcinoma.

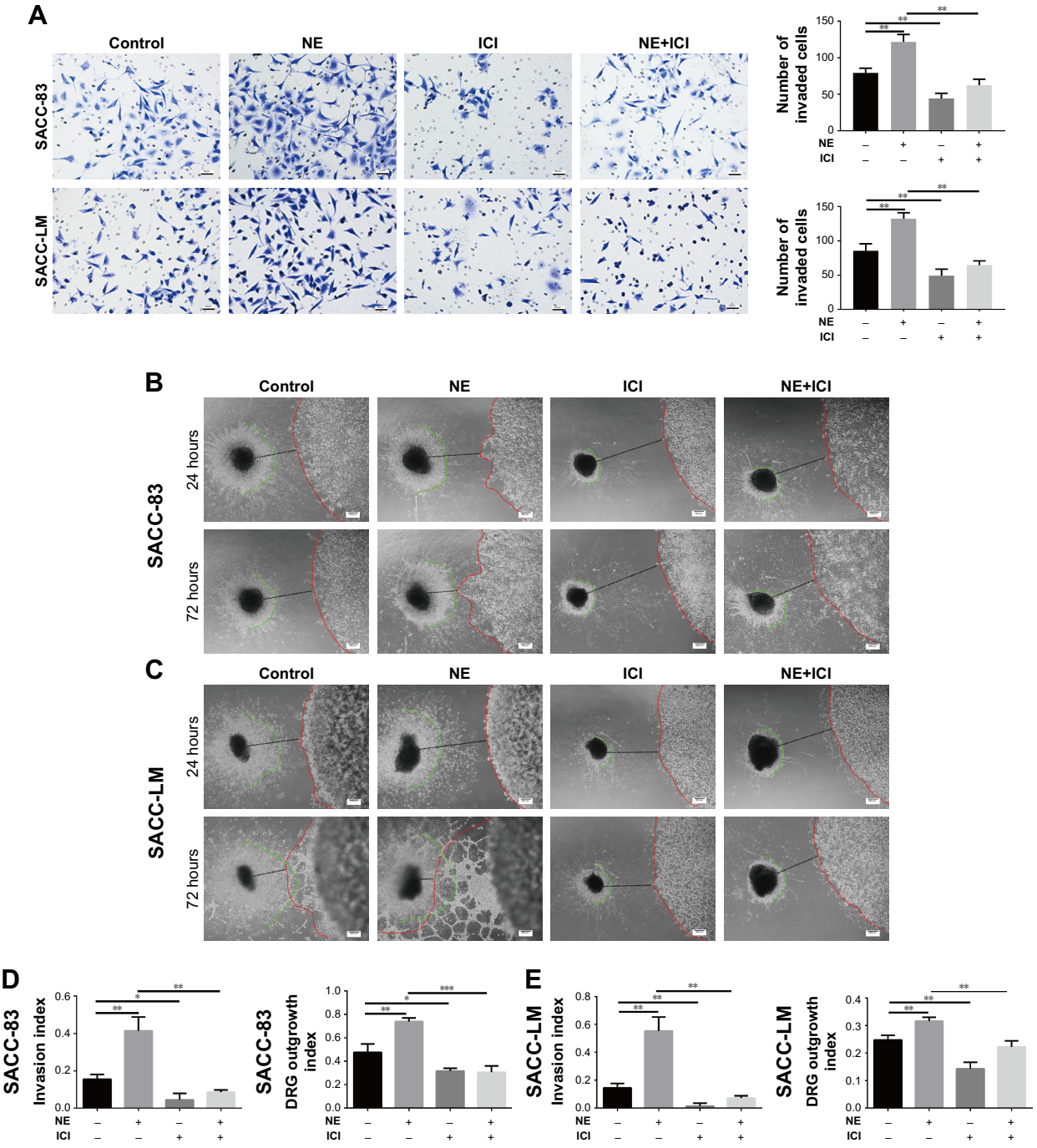

Figure 6 NE contributed to PNI in SACC via β2-AR.

Notes: (**A**) Transwell PNI assay comparing the PNI abilities of SACC-83 and SACC-LM cells treated with 10 μM NE and/or 10 μM ICI118,551, with quantification of the number of invaded cells at 24 hours. Original magnification, 200×; scale bar =50 μm. (**B**, **C**) DRG coculture models comparing the PNI abilities of SACC-83 and SACC-LM cells treated with 10 μM NE and/or 10 μM ICI118,551. The red lines indicate the edges of the SACC colonies, the green lines indicate the edges of outgrowing DRG neurites, and the black lines indicate the total distance between the DRGs and the cancer colonies. The nerve invasion index (α/γ) and DRG outgrowth index (β/γ) were calculated as described in the Materials and methods section. (**D**, **E**) The nerve invasion index and the DRG outgrowth index were quantified at 72 hours relative to that at 24 hours. Original magnification, 40×; scale bar =200 μm. *P<0.05, **P<0.01, ***P<0.001. The error bars indicate the SD.

Abbreviations: β2-AR, β2-adrenergic receptor; DRG, dorsal root ganglia; NE, norepinephrine; PNI, perineural invasion; SACC, salivary adenoid cystic carcinoma.

for SACC-LM, respectively) and NE groups (Figure 6A, P<0.01 for SACC-83 and P<0.001 for SACC-LM, respectively). To confirm the results of the Transwell PNI assay, another DRG coculture model was established to evaluate cancer–nerve interactions and to calculate the nerve invasion index and DRG outgrowth index. A colony of SACC cells was grown in Matrigel adjacent to cultured DRGs. In the 10 μM NE groups, neurite outgrowth extended from

the DRGs and projected into SACC cell colonies within 72 hours, providing an invasive pathway for the SACC cells. SACC cells that dissociated from colonies formed clusters that migrated in a unidirectional manner along the nerve toward the ganglion. Over time, tumor cells gradually formed peak-like clusters to form marked PNI phenomenon, in contrast with the control groups (Figure 6B–E, $P<0.01$ for SACC-83 and $P<0.01$ for SACC-LM, respectively). To assess the role of β2-AR in the PNI process, ICI118,551 was added to the media and we observed that neural invasion of SACC cells was markedly suppressed, compared to that in the control or 10 μM NE group (Figure 6B–E). In addition, DRG outgrowth was also accelerated by NE in comparison with control group, but was inhibited with the addition of ICI118,551 (Figure 6B–E). However, exogenously added phentolamine did not inhibit NE-induced neural invasion of SACC cells (Figure S6A and B). Moreover, the important role of β2-AR in mediating NE-induced PNI was also verified using the DRG coculture model with SACC cells that were transfected with β2-AR siRNA (Figure 7A and B). Therefore, the DRG coculture model effectively demonstrated the reciprocal interaction between SACC cells and neurites in vitro and also suggested that β2-AR plays a crucial role in both endogenous and exogenous NE-induced PNI in SACC.

NE induced EMT and upregulated MMPs via β2-AR in SACC cells

Epithelial–mesenchymal transition (EMT) plays a crucial role in regulating tumor cell migration and invasion during the progression of malignant tumors. We performed qRT-PCR and Western blot assay to investigate whether the EMT process and matrix metalloproteinase (MMP) expression levels were regulated by NE stimulation. PCR analysis demonstrated that 10 μM NE resulted in the upregulation of N-cadherin, Slug, Vimentin, MMP2, and MMP9 mRNA, whereas E-cadherin expression was downregulated (Figure 8A and B). Moreover, Western blot analysis confirmed that E-cadherin expression was reduced and that Vimentin, Slug, MMP2, and MMP9 protein expression levels were markedly increased in SACC cells treated with NE (Figure 8C–F). However, qRT-PCR and Western blot assay revealed that interruption of β2-AR signaling with ICI118,551 reversed NE-induced mesenchymal status by upregulating E-cadherin and downregulating N-cadherin, Slug, MMP2, and MMP9 (Figure 8). The above results were further verified in SACC cells transfected with β2-AR siRNA (Figure 9). Collectively, our findings suggest that NE induced EMT and upregulated MMPs via β2-AR in SACC cells.

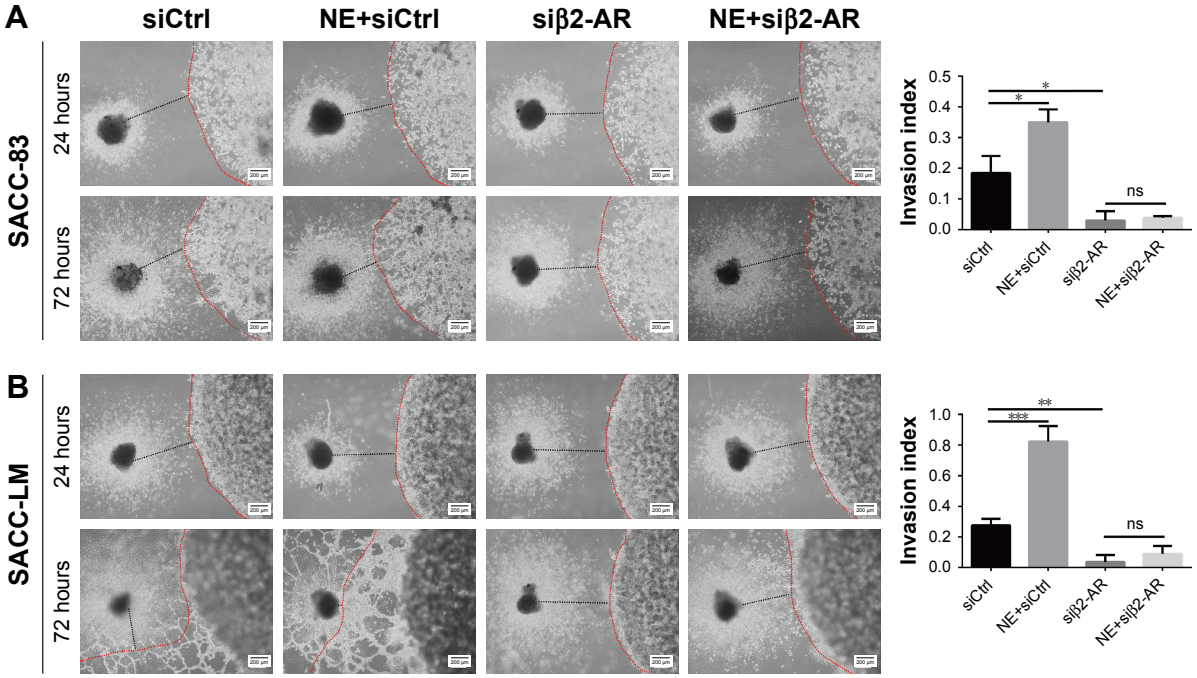

Figure 7 β2-AR mediated NE-induced PNI by SACC cells.

Notes: (**A**, **B**) DRG coculture models comparing the PNI abilities of SACC-83 and SACC-LM cells after transfection with β2-AR siRNA for 48 hours. The nerve invasion index was quantified at 72 hours relative to that at 24 hours. Original magnification, 40×; scale bar =200 μm. *$P<0.05$, **$P<0.01$, ***$P<0.001$. The error bars indicate the SD.

Abbreviations: β2-AR, β2-adrenergic receptor; DRG, dorsal root ganglia; ns, no significance; NE, norepinephrine; PNI, perineural invasion; SACC, salivary adenoid cystic carcinoma.

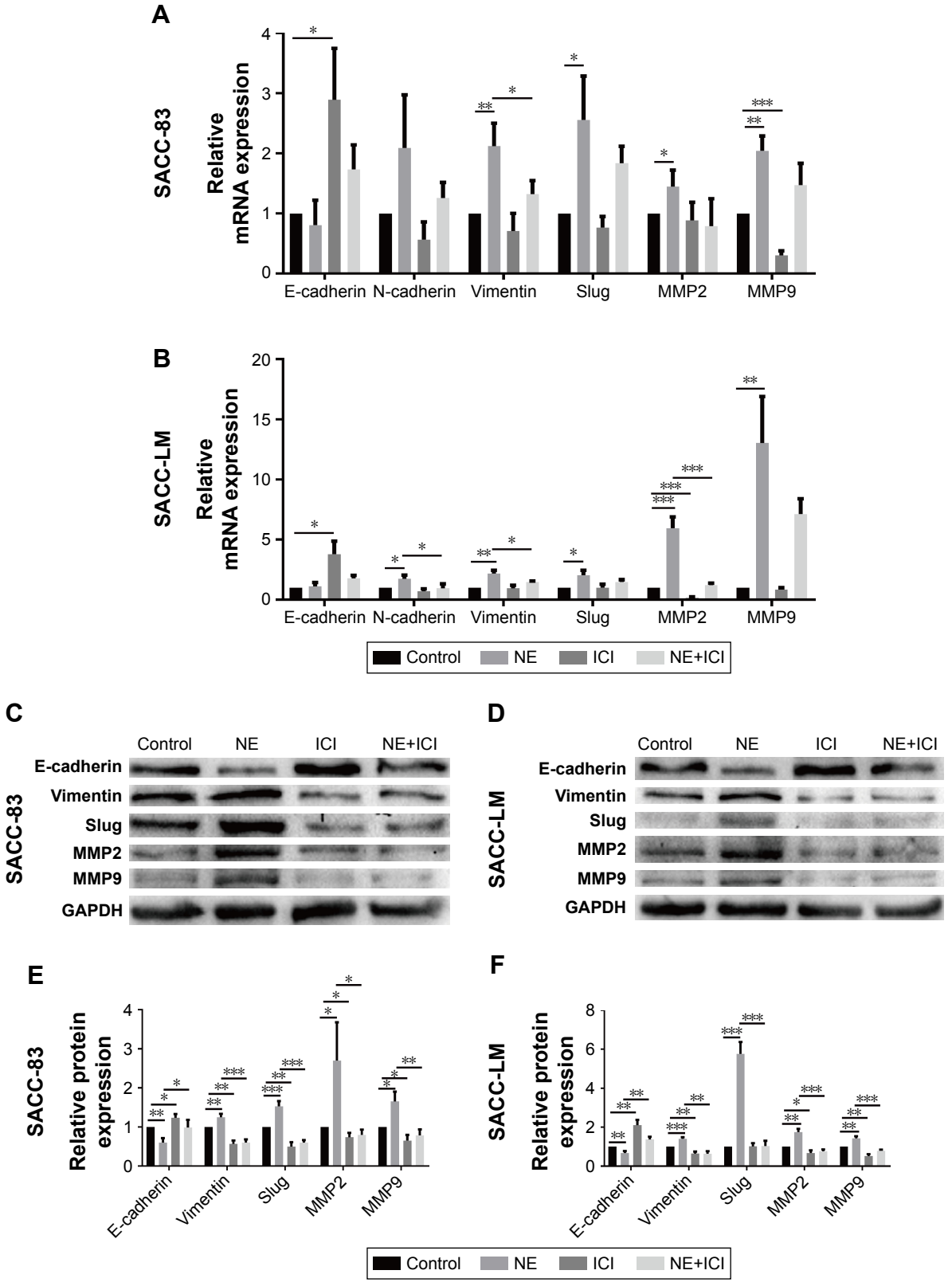

Figure 8 NE regulated the EMT and MMP expression levels via β2-AR in SACC cells.

Notes: (**A**, **B**) qRT-PCR analysis of the expression of indicated genes in SACC-83 and SACC-LM cells treated with 10 μM NE and/or 10 μM ICI118,551. GAPDH expression was detected as an internal control. The mRNA expression levels of E-cadherin, N-cadherin, Vimentin, Slug, MMP2, and MMP9 were quantified and expressed as fold-changes compared to the control groups. (**C**, **D**) Western blot analysis of the expression of the indicated proteins in SACC-83 and SACC-LM cells treated with 10 μM NE and/or 10 μM ICI118,551. GAPDH expression was detected as an internal control. (**E**, **F**) Protein expression levels in SACC-83 and SACC-LM cells were quantified and expressed as fold-changes compared with control groups. *$P<0.05$, **$P<0.01$, ***$P<0.001$. The error bars indicate the SD.

Abbreviations: β2-AR, β2-adrenergic receptor; EMT, epithelial–mesenchymal transition; GAPDH, glyceraldehyde 3-phosphate dehydrogenase; MMP, matrix metalloproteinase; NE, norepinephrine; qRT-PCR, quantitative real-time polymerase chain reaction; SACC, salivary adenoid cystic carcinoma.

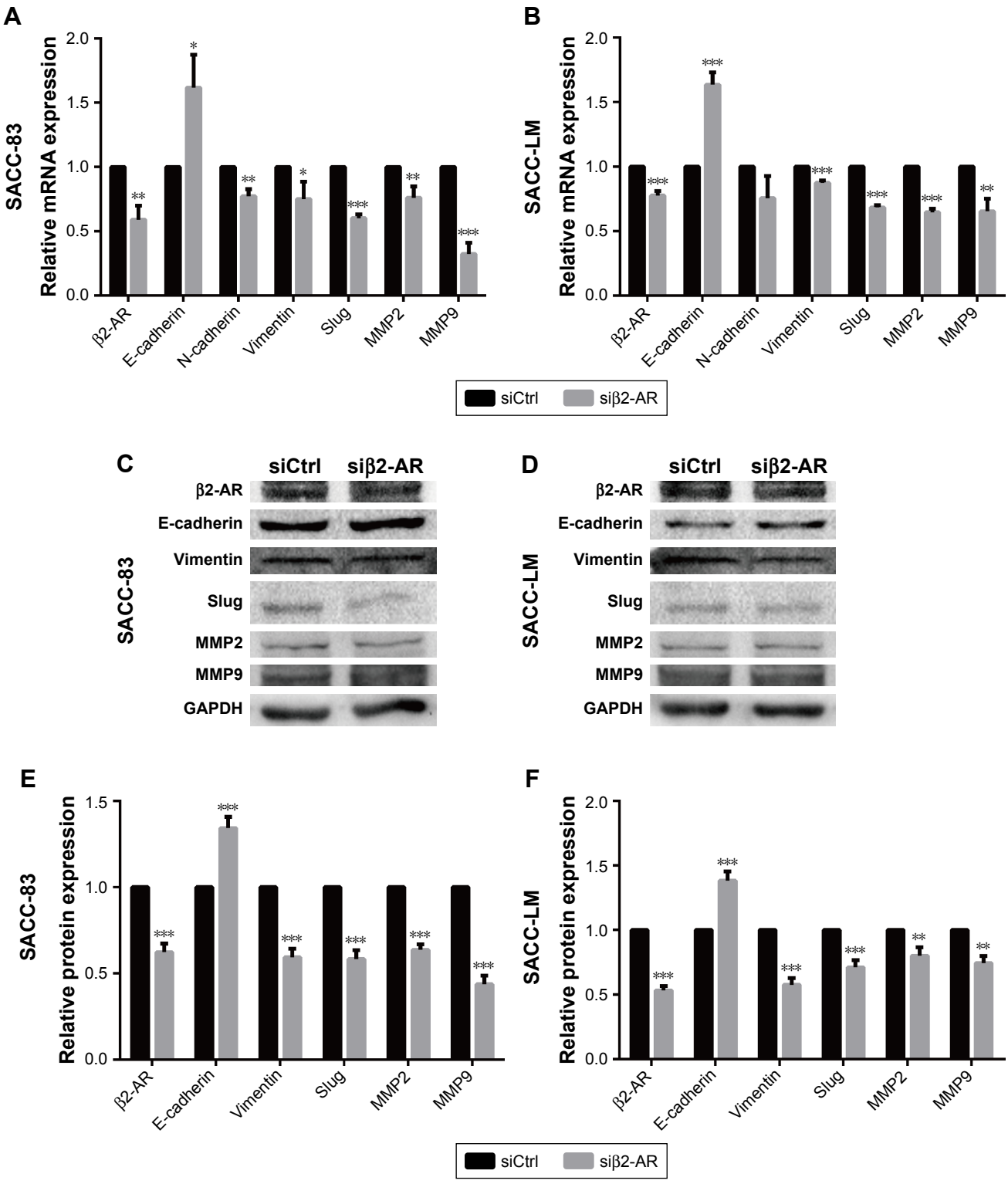

Figure 9 β2-AR mediated NE-induced EMT and upregulation of MMPs in SACC cells.

Notes: (**A**, **B**) qRT-PCR analysis of expression of the indicated genes in SACC-83 and SACC-LM cells after transfecting with β2-AR siRNA for 24 hours. GAPDH expression was detected as an internal control. The mRNA expression levels of E-cadherin, N-cadherin, Vimentin, Slug, MMP2, and MMP9 were quantified and expressed as fold-changes compared with control groups. (**C**, **D**) Western blot analysis of the expression of the indicated proteins in SACC-83 and SACC-LM cells after transfecting with β2-AR siRNA for 48 hours. GAPDH expression was detected as an internal control. (**E**, **F**) Protein expression levels in SACC-83 and SACC-LM cells were quantified and expressed as fold-changes compared with control groups. *$P<0.05$, **$P<0.01$, ***$P<0.001$. The error bars indicate the SD.

Abbreviations: β2-AR, β2-adrenergic receptor; EMT, epithelial–mesenchymal transition; GAPDH, glyceraldehyde 3-phosphate dehydrogenase; MMP, matrix metalloproteinase; NE, norepinephrine; qRT-PCR, quantitative real-time polymerase chain reaction; SACC, salivary adenoid cystic carcinoma.

Discussion

SACC is notorious for PNI. PNI involves a complex reciprocal interaction between the tumor microenvironment and cancer cells. PNI enables tumor cells to disseminate along nerve fibers, which causes enormous difficulty for surgeons when attempting to resect tumors completely and results in local recurrence and poor prognosis. However, there are no effective therapeutic strategies for PNI to date. Our research group has focused on PNI in SACC for nearly 20 years, and we have investigated possible pathogenic mechanisms of PNI in SACC such as Schwann-like cell differentiation,[28,29] nerve growth factor,[30] and the involvement of chemokine (C-C motif) ligand 5/C-C chemokine receptor type 5.[13,31] Recently, the sympathetic nervous system was proposed to play a vital role in cancer initiation and progression.[14,15] Given that sympathetic nerve fibers richly innervate salivary gland tissues, we aimed to determine whether the sympathetic system regulates PNI in SACC.

In this study, we discovered that sympathetic innervation, β2-AR, and NE were distributed in SACC tissues and correlated positively with PNI, supporting the presence of a functional sympathetic system in PNI in SACC. β2-AR was also overexpressed in SACC cell lines. In addition, the sympathetic neurotransmitter NE promoted proliferation, migration, and PNI by activating β2-AR (Figure 10). Subsequently, we found that NE/β2-AR signaling may promote proliferation, migration, and PNI by SACC cells by inducing EMT and upregulating MMPs. However, β2-AR inhibition by a specific antagonist or siRNA abrogated NE-induced PNI. In summary, our findings reveal the supportive role of sympathetic innervation in the pathogenesis of SACC PNI and suggest β2-AR as a potential therapeutic target for treating PNI in SACC.

In recent years, the importance of the sympathetic system in the tumor microenvironment has gradually become increasingly recognized. In this study, we found that the sympathetic innervation density in SACC was markedly higher than in NSG tissues and positively correlated with the M category and PNI. The increased sympathetic innervation enables tumor cells to have a greater chance to invade and disseminate along nerve fibers. However, an increased number of sympathetic nerve fiber ends enhance the reciprocal interactions between tumor cells and nerve fibers by delivering the neurotransmitter NE. The significant role of NE in promoting PNI by SACC cells was further confirmed by our DRG coculture models. Although a previous study demonstrated that sympathetic innervation in peritumor tissues positively correlated with prostate cancer recurrence,[15] the present study reveals that sympathetic nerve fibers densely innervate SACC tumor tissues. Perhaps tumor cells

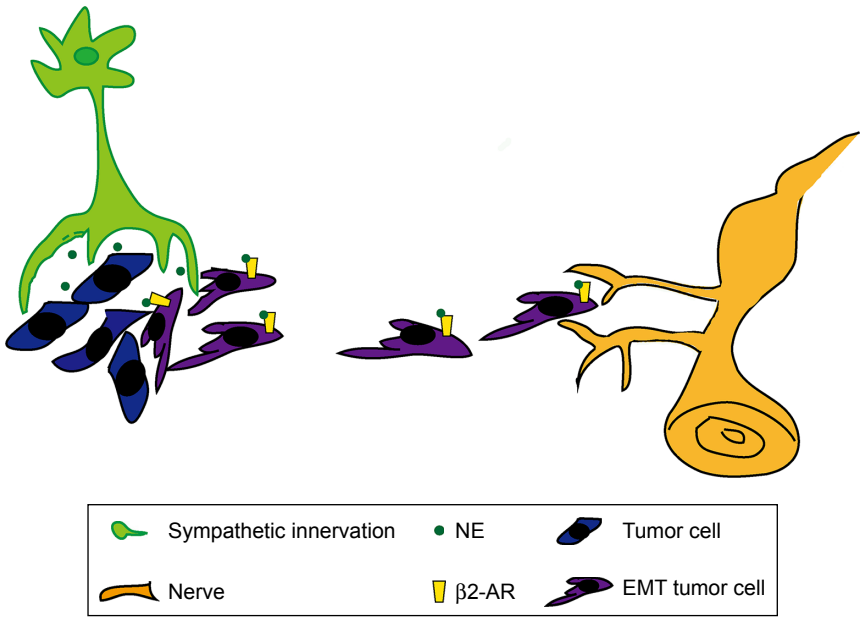

Figure 10 Schematic illustration showing how sympathetic innervation contributes to PNI in SACC.
Notes: Sympathetic nerve fibers innervate SACC tissues and deliver the sympathetic neurotransmitter NE into the tumor microenvironment. NE induces EMT of SACC cells and further promotes proliferation, migration, and PNI of SACC cells by activating β2-AR in tumor cells.
Abbreviations: β2-AR, β2-adrenergic receptor; EMT, epithelial–mesenchymal transition; NE, norepinephrine; PNI, perineural invasion; SACC, salivary adenoid cystic carcinoma.

attracted sympathetic neurite outgrowth from peritumor tissues into the tumor microenvironment by delivering neurotrophic factors.[21] Moreover, tumor cell invasion of nerve fibers may lead to nerves appearing larger than normal. Because sympathetic innervation in peritumor tissues could markedly accelerate the progression of prostate cancer, we suggest that sympathetic innervation in SACC with PNI should play a much more important role in tumor progression. Given the correlation between sympathetic innervation and distant metastasis or PNI in SACC, it is promising to develop therapeutic strategies based on local sympathectomy.

Adrenergic receptors are important members of a functional sympathetic system, and the effects of the sympathetic neurotransmitter NE are mediated by α-ARs and β-ARs. β-ARs are mainly composed of the β1-AR, β2-AR, and β3-AR subtypes, among which β2-AR was reported to play a central role in tumor initiation and metastasis.[32–35] Our current study showed that β2-AR was overexpressed in SACC with PNI in comparison with SACC without PNI or NSG tissues. β2-AR also proved to be correlated with the TNM stage, suggesting an important role for β2-AR expression in SACC progression. Furthermore, we examined the expression levels of both α-ARs and β-ARs by qRT-PCR and immunofluorescence assay and confirmed β2-AR overexpression in SACC cells. Here, we investigated the important role of β2-AR in mediating NE-induced proliferation, migration, and PNI. Unlike our study, a previous report provided evidence that β2-AR was negatively expressed on SACC cells in spite of NE-induced proliferation and migration of SACC cells.[36] We propose that differences in the SACC cell lines, β2-AR primer sequences, and primary β2-AR antibodies used may account for the different results. Given the dense sympathetic innervation in SACC with PNI and secretion function of sympathetic nerve ends, we speculated that the sympathetic neurotransmitter NE concentration is also high in SACC with PNI. As expected, this speculation was confirmed by ELISA data generated in this study. Moreover, previous studies showed that the intratumor NE concentration was higher than that in the blood,[37,38] suggesting that the main source of NE was indeed from local sympathetic innervation. Our results were consistent with previous reports showing higher NE levels in human ovarian carcinoma and pancreatic cancer than in normal tissues.[37,39] Furthermore, NE-induced proliferation, migration, and PNI were confirmed experimentally in this study. In addition, we found that NE was expressed in the culture supernatant of DRG coculture models, DRG, and SACC cells, where the NE concentration peaked in the DRG coculture model with PNI. We suspected that NE expressed in supernatant of DRGs may have been secreted by neurite outgrowths from DRGs. In contrast, NE expressed in the supernatant of SACC cells indicated that NE may have been auto-synthesized by SACC cells. Auto-synthesis of neurotransmitters has also been reported in breast cancer cells and pancreatic cancer cells.[19,40] We previously reported that SACC cell differentiation into Schwann-like cells was associated with PNI. Similarly, we propose that SACC cells may also attain the ability to differentiate into neuro-like cells capable of secreting neurotransmitters like NE. In addition to endogenous NE from DRG and SACC cells, overexpression of NE in DRG coculture models with PNI suggested that PNI may contribute to NE secretion. It is possible that neurite outgrowths from DRGs invaded by cancer cells secreted much more NE in response to injury.[11] Therefore, our ELISA results obtained with clinical SACC tissues and DRG coculture models jointly suggest that NE may contribute to PNI in SACC.

Proliferation and migration abilities are two basic characteristics of malignancies. Only SACC cells with exuberant vitality and strong mobility can survive and metastasize to distant sites. We found that NE promoted the proliferation and migration of SACC cells in a dose-dependent manner, whereas the β2-AR antagonist ICI118,551 effectively blocked these effects. Moreover, ICI118,551 also inhibited the proliferation and migration of SACC cells in control groups. However, nonselective α-AR blocker phentolamine failed to abrogate the NE-dependent increase in the proliferation and migration of SACC cells, suggesting that NE-induced proliferation and migration were not mediated by α-AR. Combined with previous ELISA results that NE might be auto-synthesized by SACC cells, we can conclude that functional sympathetic signaling occurs in SACC cells and that both endogenous and exogenous NE promoted the proliferation and migration of SACC cells, which could be abrogated by ICI118,551. Our findings were partly consistent with previous findings showing that NE promoted the proliferation and migration of both oral squamous cell carcinoma cells and SACC cells.[36] However, we further investigated the vital role of β2-AR in mediating NE-induced proliferation and migration, and the role of autocrine NE in the progression of SACC cells. Several studies have also shown that neurotransmitters could be auto-synthesized by cancer cells and delivered into the tumor microenvironment to promote tumor growth and mobility,[19,40] suggesting that autocrine sympathetic signaling may generally exist in different cancer cells.

PNI is a prominent characteristic of neurotropic tumors. Recently, several studies have focused on the reciprocal interaction between tumor cells and nerve fibers in PNI.[6,11] Given the dense sympathetic innervation and high NE

concentration in SACC with PNI, we sought to determine whether NE contributes to PNI progression in SACC. Our results showed that NE promoted PNI by SACC cells in a dose-dependent manner, which could be abrogated by ICI118,551. However, phentolamine failed to inhibit NE-induced neural invasion of SACC cells, suggesting that NE-induced neural invasion was not mediated by α-AR. Combining PNI results with previous ELISA results, we can conclude that both endogenous NE from DRG and SACC cells, and exogenously added NE significantly contributed to PNI by SACC cells via β2-AR. Moreover, both the nerve invasion index and DRG outgrowth index increased during PNI progression, further suggesting that PNI results from reciprocal interactions between tumor cells and nerve fibers. Perhaps tumor cells attracted neurite outgrowth from DRGs by secreting neurotrophic factors into the microenvironment.[21] In addition, inhibition of β2-AR by siRNA or treatment with ICI118,551 abrogated NE-induced PNI, suggesting that β2-AR mediated NE-induced PNI in SACC cells. Increasing epidemiologic evidence has shown that cancer patients taking β-blockers may have a better prognosis.[18,20] Given that β-blockers have already been widely used as therapy for cardiovascular diseases for decades,[34] it should be safe and acceptable if β-blockers can be used as an adjuvant treatment of SACC PNI. Therefore, blockade of β2-AR may represent a potential therapeutic strategy for PNI in SACC.

EMT is an important transformation that helps tumor cells achieve malignant behavior. MMPs are capable of degrading extracellular matrix proteins, which play a vital role in tumor invasion and metastasis. Both EMT and MMPs have been associated with PNI in SACC.[41,42] Our previous study revealed that p53 downregulation promoted PNI by SACC cells by inducing EMT.[43] Moreover, previous data showed that NE enhanced PNI of pancreatic cancer cells by activating STAT3 and upregulating MMPs, whereas treatment with ICI118,551 or propranolol significantly blocked the NE-induced PNI effect.[21] In this study, we found that NE induced EMT and upregulated MMP2 and MMP9 expression. However, inhibiting β2-AR with either an antagonist or siRNA blocked the NE-induced EMT and upregulation of MMPs. Considering the NE-induced proliferation, migration, and PNI results, we can speculate that NE/β2-AR signaling may promote proliferation, migration, and PNI by SACC cells by regulating the EMT and MMP expression levels.

Limitations

Nevertheless, this study also has some limitations that should be noted. First, this was a retrospective study with a relatively small cohort carried out in a single institution, which may have resulted in selection bias. To overcome this limitation, additional studies comprising larger cohort from multiple centers are expected in the future. Second, β-adrenergic signaling was reported to regulate multiple molecules and pathways in tumor initiation and progression.[44] Therefore, the downstream mechanism of NE/β2-AR signaling in PNI in SACC awaits further study beyond the EMT and MMP induction. Third, although we investigated the important role of NE/β2-AR signaling in PNI in SACC in vitro, further study is required to confirm our findings in vivo.

Conclusion

The present study indicates that sympathetic innervation is positively correlated with SACC PNI and that the sympathetic neurotransmitter NE contributes to PNI by SACC cells by activating β2-AR. Our findings reveal the supportive role of sympathetic innervation in the pathogenesis of SACC PNI and suggest β2-AR as a potential therapeutic target for treating PNI in SACC. Furthermore, in addition to the sympathetic nervous system, the parasympathetic nervous system (as the other division of the autonomic nervous system) has also been proposed to play a key role in tumor progression.[15] However, whether parasympathetic nerve fibers innervate SACC has not been studied and we are currently researching the role of the parasympathetic nervous system in SACC PNI.

Acknowledgment

The present study was supported by the Key Research and Development Program of Shaanxi (grant no. 2017SF-209) and the Beijing Xisike Clinical Oncology Research Foundation (grant nos Y-HR2016-063, Y-MX2016-068, and Y-HS2017-089).

Disclosure

The authors report no conflicts of interest in this work.

References

1. Laurie SA, Ho AL, Fury MG, Sherman E, Pfister DG. Systemic therapy in the management of metastatic or locally recurrent adenoid cystic carcinoma of the salivary glands: a systematic review. *Lancet Oncol*. 2011;12(8):815–824.
2. Kokemueller H, Eckardt A, Brachvogel P, Hausamen JE. Adenoid cystic carcinoma of the head and neck – a 20 years experience. *Int J Oral Maxillofac Surg*. 2004;33(1):25–31.
3. Li Q, Huang P, Zheng C, Wang J, Ge M. Prognostic significance of p53 immunohistochemical expression in adenoid cystic carcinoma of the salivary glands: a meta-analysis. *Oncotarget*. 2017;8(17):29458–29473.
4. Ellington CL, Goodman M, Kono SA, et al. Adenoid cystic carcinoma of the head and neck: incidence and survival trends based on 1973–2007 surveillance, epidemiology, and end results data. *Cancer*. 2012;118(18):4444–4451.

5. Ni Q, Sun J, Ma C, Li Y, Ju J, Sun M. The neuropilins and their ligands in hematogenous metastasis of salivary adenoid cystic carcinoma-an immunohistochemical study. *J Oral Maxillofac Surg*. 2018;76(3):569–579.
6. Liebig C, Ayala G, Wilks JA, Berger DH, Albo D. Perineural invasion in cancer: a review of the literature. *Cancer*. 2009;115(15):3379–3391.
7. Marchesi F, Piemonti L, Mantovani A, Allavena P. Molecular mechanisms of perineural invasion, a forgotten pathway of dissemination and metastasis. *Cytokine Growth Factor Rev*. 2010;21(1):77–82.
8. Sheng L, Ji Y, Du X. Perineural invasion correlates with postoperative distant metastasis and poor overall survival in patients with PT1-3N0M0 esophageal squamous cell carcinoma. *Onco Targets Ther*. 2015;8:3153–3157.
9. Ju J, Li Y, Chai J, et al. The role of perineural invasion on head and neck adenoid cystic carcinoma prognosis: a systematic review and meta-analysis. *Oral Surg Oral Med Oral Pathol Oral Radiol*. 2016;122(6):691–701.
10. Al-Mamgani A, van Rooij P, Sewnaik A, Tans L, Hardillo JA. Adenoid cystic carcinoma of parotid gland treated with surgery and radiotherapy: long-term outcomes, QOL assessment and review of the literature. *Oral Oncol*. 2012;48(3):278–283.
11. Amit M, Na'ara S, Gil Z. Mechanisms of cancer dissemination along nerves. *Nat Rev Cancer*. 2016;16(6):399–408.
12. Larson DL, Rodin AE, Roberts DK, O'Steen WK, Rapperport AS, Lewis SR. Perineural lymphatics: myth or fact. *Am J Surg*. 1966;112(4):488–492.
13. Gao T, Shen Z, Ma C, Li Y, Kang X, Sun M. The CCL5/CCR5 chemotactic pathway promotes perineural invasion in salivary adenoid cystic carcinoma. *J Oral Maxillofac Surg*. 2018;76(8):1708–1718.
14. Cole SW, Nagaraja AS, Lutgendorf SK, Green PA, Sood AK. Sympathetic nervous system regulation of the tumour microenvironment. *Nat Rev Cancer*. 2015;15(9):563–572.
15. Magnon C, Hall SJ, Lin J, et al. Autonomic nerve development contributes to prostate cancer progression. *Science*. 2013;341(6142):1236361.
16. Zhang L, Wu LL, Huan HB, et al. Sympathetic and parasympathetic innervation in hepatocellular carcinoma. *Neoplasma*. 2017;64(6):840–846.
17. Shao JX, Wang B, Yao YN, Pan ZJ, Shen Q, Zhou JY. Autonomic nervous infiltration positively correlates with pathological risk grading and poor prognosis in patients with lung adenocarcinoma. *Thorac Cancer*. 2016;7(5):588–598.
18. Monami M, Filippi L, Ungar A, et al. Further data on beta-blockers and cancer risk: observational study and meta-analysis of randomized clinical trials. *Curr Med Res Opin*. 2013;29(4):369–378.
19. Renz BW, Takahashi R, Tanaka T, et al. β2 Adrenergic-neurotrophin feedforward loop promotes pancreatic cancer. *Cancer Cell*. 2018;33(1):75.e7–90.e7.
20. Udumyan R, Montgomery S, Fang F, et al. Beta-blocker drug use and survival among patients with pancreatic adenocarcinoma. *Cancer Res*. 2017;77(13):3700–3707.
21. Guo K, Ma Q, Li J, et al. Interaction of the sympathetic nerve with pancreatic cancer cells promotes perineural invasion through the activation of STAT3 signaling. *Mol Cancer Ther*. 2013;12(3):264–273.
22. Pagella P, Jiménez-Rojo L, Mitsiadis TA. Roles of innervation in developing and regenerating orofacial tissues. *Cell Mol Life Sci*. 2014;71(12):2241–2251.
23. Li X, Liu W, Liu J, et al. Expression of angiopoietins in central nervous system hemangioblastomas is associated with cyst formation. *Neurosci Lett*. 2017;639:120–125.
24. Livak KJ, Schmittgen TD. Analysis of relative gene expression data using real-time quantitative PCR and the 2(-Delta Delta C(T)) method. *Methods*. 2001;25(4):402–408.
25. Ayala GE, Wheeler TM, Shine HD, et al. In vitro dorsal root ganglia and human prostate cell line interaction: redefining perineural invasion in prostate cancer. *Prostate*. 2001;49(3):213–223.
26. Gil Z, Cavel O, Kelly K, et al. Paracrine regulation of pancreatic cancer cell invasion by peripheral nerves. *J Natl Cancer Inst*. 2010;102(2):107–118.
27. Xu Q, Wang Z, Chen X, et al. Stromal-derived factor-1α/CXCL12-CXCR4 chemotactic pathway promotes perineural invasion in pancreatic cancer. *Oncotarget*. 2015;6(7):4717–4732.
28. Chen W, Dong S, Zhou J, Sun M. Investigation of myoepithelial cell differentiation into Schwann-like cells in salivary adenoid cystic carcinoma associated with perineural invasion. *Mol Med Rep*. 2012;6(4):755–759.
29. Luo XL, Sun MY, Lu CT, Zhou ZH. The role of Schwann cell differentiation in perineural invasion of adenoid cystic and mucoepidermoid carcinoma of the salivary glands. *Int J Oral Maxillofac Surg*. 2006;35(8):733–739.
30. Wang L, Sun M, Jiang Y, et al. Nerve growth factor and tyrosine kinase A in human salivary adenoid cystic carcinoma: expression patterns and effects on in vitro invasive behavior. *J Oral Maxillofac Surg*. 2006;64(4):636–641.
31. Shen Z, Li T, Chen D, et al. The CCL5/CCR5 axis contributes to the perineural invasion of human salivary adenoid cystic carcinoma. *Oncol Rep*. 2014;31(2):800–806.
32. Armaiz-Pena GN, Allen JK, Cruz A, et al. Src activation by β-adrenoreceptors is a key switch for tumour metastasis. *Nat Commun*. 2013;4(1):1403.
33. Kobilka BK. Structural insights into adrenergic receptor function and pharmacology. *Trends Pharmacol Sci*. 2011;32(4):213–218.
34. Tang J, Li Z, Lu L, Cho CH. β-Adrenergic system, a backstage manipulator regulating tumour progression and drug target in cancer therapy. *Semin Cancer Biol*. 2013;23(6 Pt B):533–542.
35. Vandewalle B, Revillion F, Lefebvre J. Functional beta-adrenergic receptors in breast cancer cells. *J Cancer Res Clin Oncol*. 1990;116(3):303–306.
36. Shang ZJ, Liu K, Liang DF. Expression of beta2-adrenergic receptor in oral squamous cell carcinoma. *J Oral Pathol Med*. 2009;38(4):371–376.
37. Lutgendorf SK, Degeest K, Dahmoush L, et al. Social isolation is associated with elevated tumor norepinephrine in ovarian carcinoma patients. *Brain Behav Immun*. 2011;25(2):250–255.
38. Lutgendorf SK, Degeest K, Sung CY, et al. Depression, social support, and beta-adrenergic transcription control in human ovarian cancer. *Brain Behav Immun*. 2009;23(2):176–183.
39. Schuller HM, Al-Wadei HA, Majidi M. GABA B receptor is a novel drug target for pancreatic cancer. *Cancer*. 2008;112(4):767–778.
40. Shi M, Liu D, Duan H, et al. The β2-adrenergic receptor and HER2 comprise a positive feedback loop in human breast cancer cells. *Breast Cancer Res Treat*. 2011;125(2):351–362.
41. Wu B, Wei J, Hu Z, et al. Slug silencing inhibited perineural invasion through regulation of EMMPRIN expression in human salivary adenoid cystic carcinoma. *Tumor Biol*. 2016;37(2):2161–2169.
42. Yang X, Zhang P, Ma Q, et al. EMMPRIN silencing inhibits proliferation and perineural invasion of human salivary adenoid cystic carcinoma cells in vitro and in vivo. *Cancer Biol Ther*. 2012;13(2):85–91.
43. Yang X, Jing D, Liu L, et al. Downregulation of p53 promotes in vitro perineural invasive activity of human salivary adenoid cystic carcinoma cells through epithelial-mesenchymal transition-like changes. *Oncol Rep*. 2015;33(4):1650–1656.
44. Cole SW, Sood AK. Molecular pathways: beta-adrenergic signaling in cancer. *Clin Cancer Res*. 2012;18(5):1201–1206.